Available online at www.sciencedirect.com
ScienceDirect
Polymer 48 (2007) 2338–2344
polymer
www.elsevier.com/locate/polymer

Formation of deformed honeycomb-patterned films from fluorinated polyimide

Ye Tian [a], Shuang Liu [b], Huaiyu Ding [a], Lihua Wang [a,*], Biqian Liu [a], Yanqiao Shi [a]

[a] Laboratory of New Materials, Institute of Chemistry, The Chinese Academy of Sciences, Beijing 100080, PR China
[b] Division of Physical-Chemical Analytical Lab, Beijing Institute of Aeronautical Materials, Beijing 100095, PR China

Received 21 September 2006; received in revised form 2 February 2007; accepted 13 February 2007
Available online 15 February 2007

Abstract

Fabrication of honeycomb-patterned films from one of the soluble fluoro-polyimides in a humid atmosphere was reported in this paper. This polyimide was synthesized from 2,2′-bis(3,4-dicarboxyphenyl)hexafluoropropane dianhydride (6FDA) and 4,4′-methylene dianiline (MDA) by two-step method. The obtained polyimide kept excellent rigidity and thermal stability, and especially, exhibited good solubility both in strong bipolar solvents and in common organic solvents. By blowing airflow across the surface of the deposited solution horizontally, the pores locating at the windward side of the film could change their morphologies from circle to ellipse, while the pores at the leeward side were almost kept their shapes. A detailed research about the pore deformation on various regions in a same film was carried out. At last, the differences in pattern formation between dynamic and static environment were tested, and the results showed that pores fabricated under flowing atmosphere were smaller and more regular than those formed under static condition.

Keywords: Honeycomb pattern; Soluble fluoro-polyimide; Deformed pore morphology

1. Introduction

Microporous films with honeycomb structures have attracted great interest due to their potential applications in chemical sensors [1], optical apparatus [2], biology [3], tissue engineering [4], and micrographics [5], etc. Recently, François et al. reported a new method of using water microspheres as templates to fabricate ordered porous structures [6–9]. They cast the solution of polystyrene–polyparaphenylene block copolymer in carbon disulfide onto a substrate in a high humid atmosphere. After the solvent and water droplets evaporated completely, a film with regular honeycomb pores was formed. For the convenience of manipulation, this method aroused much attention. Many polymer materials have been used to prepare honeycomb-like films, which includes rod–coil block copolymers [10,11], star polymers [12], dendritic copolymers [13,14], amphiphilic copolymers [15–17], hydrophobic polymers [18,19], etc.

Aromatic polyimide (PI) materials have been widely researched for the past decade due to their excellent dielectric, thermal, adhesive and dimension stability, etc. [20–23]. However, most commercial polyimides are usually insoluble in common organic solvents which limits their extensive application. For this reason, it is difficult for them to fabricate honeycomb patterns using water droplets as templates. Yabu et al. [24] solved this problem by using poly(amic acid)s/polyion complex to prepare honeycomb films in highly humid atmosphere and then by imidization of poly(amic acid)s to obtain polyimide films. However, imidization is a chemical treatment, which destroys the previous structures of the films. If one kind of soluble polyimides is used to directly fabricate regular porous films in humid atmosphere, the imidization process can be avoided. Semifluorinated polyimides are the suitable PIs due to their good solubility in organic solvents without forfeiture of thermal stability, etc. [25–30]. The industrialization of 6FDA greatly promotes the development of

* Corresponding author. Tel.: +86 10 6265 0812; fax: +86 10 6255 9373.
E-mail address: wanglh@iccas.ac.cn (L. Wang).

0032-3861/$ - see front matter © 2007 Elsevier Ltd. All rights reserved.
doi:10.1016/j.polymer.2007.02.028

semifluorinated polyimide. Utilizing 6FDA as the monomer to polymerize polyimides is popular in recent years.

In the present study, we synthesized one of the soluble semifluorinated polyimides from 6FDA and MDA. The structure of the fluorinated polyimide was characterized by FT-IR, ^{1}H NMR and ^{19}F NMR. Then, 6FDA–MDA/$CHCl_3$ solutions were cast on glass substrates to form honeycomb films. By blowing airflow across the surface of the deposited solution horizontally, the pore structures can be deformed from circle to ellipse. Moreover, the differences in pattern formation between dynamic and static environment were also tested.

2. Experimental

2.1. Materials

2,2′-Bis(3,4-dicarboxyphenyl)hexafluoropropane dianhydride (6FDA) (99%, Fluoro Chemical Co.) was recrystallized from acetic anhydride before use. 4,4′-Methylene dianiline (MDA) (98%, Beijing Chemical Reagent Co.) was recrystallized from ethanol. Commercially available solvents, *N*,*N*-dimethylformamide (DMF), *N*-methyl-2-pyrrolidinone (NMP), *N*,*N*′-dimethylacetamide (DMAc), dimethyl sulphoxide (DMSO), tetrahydrofuran (THF), chloroform ($CHCl_3$), acetone and methanol (MeOH) were purchased from Beijing Chemical Reagent Corporation, and were of analytical grade. DMF was purified on distillation under reduced pressure over CaH_2 and stored over molecular sieves (4 Å). Water was purified by a Millipore system (Milli-Q, Millipore). Acetic anhydride and triethylamine (TEA) were used as received (analytical grade, Beijing Chemical Reagent Co.).

2.2. The synthesis of 6FDA–MDA

6FDA–MDA was synthesized from the two-step route. To a completely dried three-necked flask, equipped with a stirrer and a N_2 inlet, was added a solution of MDA in DMF and then 6FDA was added all at once. The mole ratio and solid content of 6FDA/MDA mixture were 1:1 and 10 wt%, respectively. The mixture reacted for 8 h at room temperature in N_2 atmosphere, yielding a viscous poly(amic acid) solution. The chemical imidization was carried out with acetic anhydride (the dehydration reagent) and TEA (the catalyzer) at room temperature for 10 h. The reaction mixture was then added to ethanol solution. The precipitate was collected by filtration, washed with water, and dried in vacuum at 160 °C to obtain the solid of the fluorinated polyimide.

2.3. Film preparation

6FDA–MDA was dissolved in $CHCl_3$ at first, and then, the polymer solution was put into two different types of humid environment: the static and the dynamic environments. In static environment, the polymer solution was directly cast on glass substrates at room temperature in a chamber whose relative humidity could be controlled. In dynamic environment, moist airflow through a tube with a diameter of 4.0 mm blew across (the velocity of the moist airflow was ~20 to 60 m/min) the surface of the polymer solution under ambient conditions (70–95% relative humidity). After the solvent evaporated completely, the films were obtained.

2.4. Measurements

GPC analysis of the polymer was performed using THF as the eluant. Fourier transform infrared spectroscopic (FT-IR) analysis was performed on Nicolet IR560 spectrometer. ^{1}H NMR and ^{19}F NMR spectra were performed using a Varic ECA-600 spectrometer using DMSO-d_6 as the solvent. Thermogravimetric analyses (TGA) were performed on a TGA-2050 thermal analyzer using a heating rate of 20 mL/min in N_2. The glass transition temperature was determined by differential scanning calorimetry (Seiko DSC200) from 100 to 400 °C at the heating rate of 10 K/min. Mechanical properties of the film were measured on a TS-2000 at room temperature with film specimens at the rate of 5 mm/min. The solubility was determined by dissolving 1 g of 6FDA–MDA in 9 g of solvent (10 wt%) at room temperature, with mechanically stirring in nitrogen for 24 h.

The surface morphologies of the microstructured films were characterized by scanning electron microscopy (SEM, JEOL SEM4500, Tokyo, Japan) carried out at a 30-kV accelerating voltage.

3. Results and discussion

3.1. Polymer characterization

6FDA–MDA was successfully polymerized by the conventional two-step polymerization method, involving ring-opening polyaddition forming poly(amic acid) and subsequently chemical cyclodehydration using acetic anhydride as dehydration reagent and TEA as the catalyzer. The chemical structure and schematic synthetic route of this polymer are shown in Scheme 1.

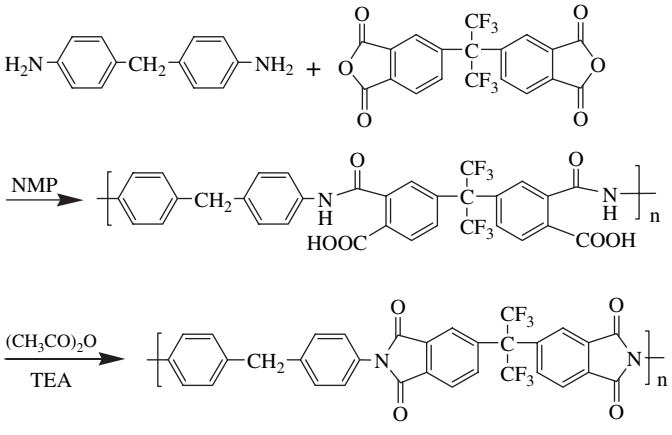

Scheme 1. Synthetic route for 6FDA–MDA.

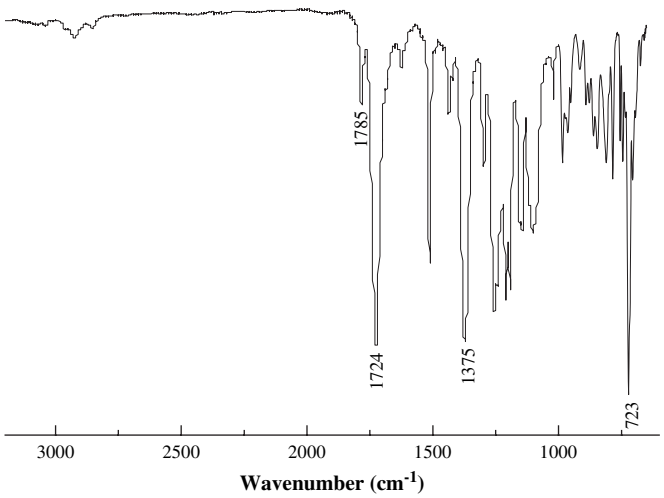

Fig. 1. FT-IR spectrum of 6FDA–MDA.

Fig. 1 shows the FT-IR measurement for the 6FDA–MDA. It can be seen that the absorptions at about 1780 and 1720 cm^{-1} assigned to the asymmetric and symmetric C=O stretching vibrations in imide groups, and the absorption at about 1370 cm^{-1} attributed to C–N stretching vibration, were the characteristic absorption bands of a polyimide, whereas no characteristic absorptions of a poly(amic acid) at around 3363 cm^{-1} (N–H stretching vibration) and 1650 cm^{-1} (amide C=O stretching vibration) were found. These results indicate that polyimide is well imidized.

^{1}H NMR measurement (Fig. 2) showed that the aromatic protons were detected at around 7.3–8.1 ppm, depending on the position in the aromatic ring. The $-CH_2$ group was in the 4.2 ppm and the aromatic carboxylic acid proton and aromatic amide proton peak (10.5 ppm) completely disappeared, which meant that the poly(amic acid) was completely converted into polyimide. In ^{19}F NMR analysis (Fig. 3), a sharp single peak was observed at −63.11 ppm, also providing evidence for the successful synthesis of 6FDA–MDA.

The GPC analysis based on linear polystyrene (PSt) standards gave a weight-average molecular weight (M_w) of 165 200 and a relatively narrow polydispersity (M_w/M_n) of 1.79 for 6FDA–MDA (Table 1). The thermal properties of 6FDA–MDA were characterized using differential scanning calorimetry (DSC) for testing the glass transition temperature (T_g) and TGA for the decomposition temperature (T_d). Thermal behaviour data of 6FDA–MDA are summarized in Table 1. The glass transition temperature (T_g) was 283 °C, demonstrating the excellent rigidity of 6FDA–MDA. The TGA analyses showed 10 wt% loss of 6FDA–MDA at 523 °C, exhibiting its good thermal stability. Mechanical properties of the film are also showed in Table 1. The 6FDA–MDA flat film was obtained by casting polymer solutions on glass surface followed by thermal baking to remove the solvents. The results showed that the 6FDA–MDA film had the tensile strength (T_s) of 105.6 MPa, and the elongations (E_b) at breakage of 7.5%. The tensile modulus (T_M) was measured as 1.22 GPa, indicating that the polymer films were tough and strong materials.

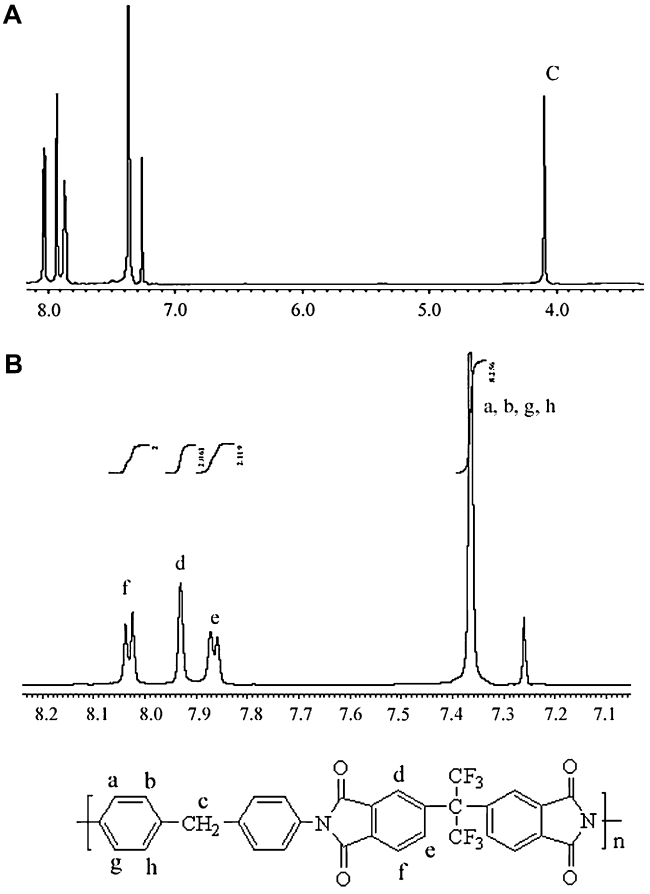

Fig. 2. ^{1}H NMR spectrum of 6FDA–MDA.

The solubility was determined by dissolving 1 g of 6FDA–MDA in 9 g of solvent (10 wt%) at room temperature. Table 2 summarizes its solubility. It can be seen that the 6FDA–MDA exhibited good solubility in common organic solvents such as NMP, DMAC, DMF and DMSO, THF, $CHCl_3$ and acetone. The good solubility of the polymers could be interpreted by the introduction of trifluoromethylphenyl group and the bulk pendant phenyl group in the polymer backbone, which

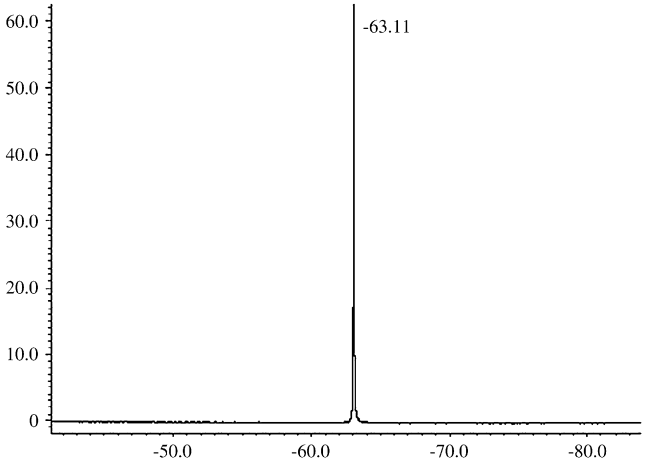

Fig. 3. ^{19}F NMR spectrum of 6FDA–MDA.

Table 1
Thermal and mechanical properties of 6FDA–MDA

Polymer	M_w	M_w/M_n	T_g (°C)	T_d (°C)	T_s (MPa)	T_M (GPa)	E_b (%)
6FDA–MDA	165 200	1.79	283	523	105.6	1.22	7.5

Table 2
Solubility of the 6FDA–MDA in different solvents

Solvents	6FDA–MDA
NMP	+
DMAc	+
DMF	+
DMSO	+
THF	+
Acetone	+
$CHCl_3$	+
MeOH	−

+ soluble; − insoluble.

induced the decrease of the interaction of polymer chain. We have reported before that the good compatibility between the polymers and their solvents was beneficial to the formation of regular structures [31,32]. This good solubility of 6FDA–MDA in organic solvent provided the precondition for the formation of the regular patterns.

3.2. Deformation of the honeycomb structures under dynamic environment

In previous studies, most results have showed circular or hexagonal pores, restricted by the shape of water droplets. However, Nishikawa et al. [33] changed the pore shapes from hexagon to rectangle, square, or triangle based on stretching of a viscoelastic polymer film after the honeycomb mesh had been formed. They thought these kinds of pores could satisfy the different requirements, such as cell culture, tissue engineering or many other areas. Li et al. [34] set the airflow with a certain angle with the normal of the solution surface, and blew to the solution surface, changing pore morphology from circle to ellipse. In our study, humid airflow horizontally crossed the solution surface with the controlled velocity. Different parts of the film were characterized by SEM to investigate the influence of airflow for the whole film. 6FDA–MDA was dissolved in $CHCl_3$, and then cast on a glass slide. Moist airflow, namely nitrogen gas bubbled through distilled water, blew across the solution surface horizontally through a tube with a diameter of 4.0 mm. Immediately, the $CHCl_3$ began to evaporate and some phenomena were observed. It could be easy to see the transparent polymer solution becoming turbid due to emulsification. When the solvent evaporated completely, an opaque film left.

Fig. 4 shows optical photo of the film and SEM images of the pore structures under airflow velocity of 20 m/min. The figure also shows the schematic illustration of the deformation process of the dropped solution. The left side of the showed film is the windward side, and the right side is the leeward side. The pore structures characterized by SEM are all located at the windward side. As can be seen from Fig. 4 all the pores are deformed their shapes from circle to ellipse (the aspect ratios of the elliptic pores are about 1.20). However, their deformed direction is not uniform, which parallels the brim of the film. The change of the pore shapes was due to the blowing of the airflow. Airflow gave the dropped solution a horizontal shear, which caused the solution to tend to move along with airflow. However, when the flowing rate was 20 m/min, this force was too weak to overcome the adhered resistance between the solution and the substrate. Only small windward part of the solution could move sideward where they had less resistance. Therefore, the morphology of the dropped solution varied slightly from circle to ellipse. The water droplets condensed on windward part of the solution surface accordingly received a stretched force derived from the deformation of the dropped solution, and changed their shapes following this force. The deformed direction of the pores, consequently, was not uniform.

The pores in the leeward side (right side) of the film are hardly influenced by the airflow because of the adhered resistance force, and their morphology nearly has no change (see Fig. 5B).

In order to further study the influence of airflow velocity, the velocity was increased to 60 m/min. Fig. 5 shows optical photo of the film and the SEM images of the pore structures. It can be found from the optical photo that the deformation degree of the film is larger than that prepared at 20 m/min, owing to the large shear force. Moreover, the SEM images clearly describe the deformation tendency of the pores. The pores in the windward side (left side) of the film changed from circle to ellipse with the aspect ratio of 1.70, while the leeward side (right side) pores hardly deform their shapes (the aspect ratio is 1.06). The reason was that the condensed water droplets in left side received a strong shear that forced them to be deformed from circle to ellipse following the airflow direction. However, the strength of this shear was rapidly decreased when it reached to the right side of the solution due to the resistance mentioned above. Therefore, this part of the solution receives little outside force, and the pore shapes hardly change.

In addition, it also can be seen in Fig. 5 that, a two-dimension structure is formed in the left side of the film (Fig. 5A), and a multilayer structure is obtained in the right side (Fig. 5B). This phenomenon should be caused by the different thickness of these two parts. In present study, the strong shear force caused the solution to concentrate to the leeward side, which led to the thickness of the windward side of the solution becoming much thinner than that of the leeward side. Previous researches had showed some factors on forming a 2D or 3D pore structures. Srinivasarao et al. [35] pointed out that when a solvent less dense than water is used, such as benzene or toluene, 3D array could be produced. Otherwise, only a single layer of pores could be formed. Bolognesi et al. [36] thought whether the structure was a single layer or a multilayer was depended on the surface tension of solvent (γ_s) and water (γ_w), as well as the interface tension between the solvent and water ($\gamma_{w/s}$). The depth of water droplets

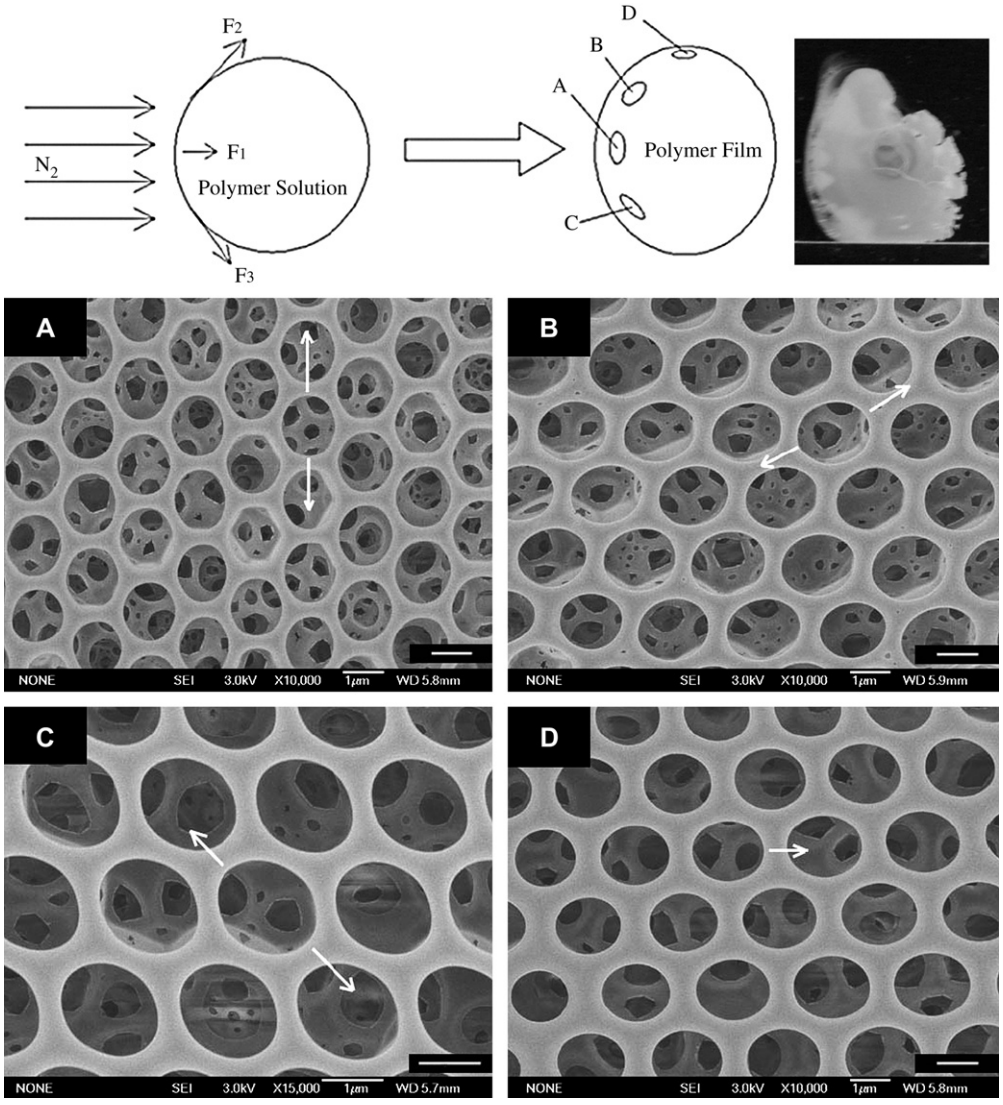

Fig. 4. SEM images of the deformed honeycomb structures at the blowing velocity of 20 m/min. Conditions: temperature, 25 °C; concentration, 2 g/L; spreading volume, 100 μL. The aspect ratio of the elliptic pores is A 1.20, B 1.20, C 1.21, D 1.15. The scale bar is 1 μm.

immerging into solution (z) could be estimated by the following equation, $z = [R(\gamma_w - \gamma_{w/s})]/\gamma_s$, where R was the radius of the water droplet. In our opinion, the dimensionality of the pore structures also could be influenced by the thickness of the liquid film. If the thickness was too thin, no space would be left for water droplets to immerge. However, if the thickness was thick enough, even though the solvent is more dense than water, the water droplets on the surface still had space to penetrate into the inside of the liquid film, driven by the press of the subsequent condensed ones and formed 3D structures. As a result, after the dropped solution solidified completely, the left side remained as a single layer structure, while the right side obtained a 3D pattern. We also noticed that the inside layers of the 3D pattern were not regular (Fig. 5B). This was because when water droplets were forced to be pushed into the inside of the liquid film, the growth and the array of the droplets ceased due to strong resistance inside, leading to an irregular pattern.

3.3. Differences in pattern formation between dynamic and static environment

6FDA–MDA/$CHCl_3$ solutions were put in two different types of humid atmospheres to form regular porous films: the static environment and the dynamic environment with the blowing rate of 20 m/min. It needs only 70–80 s for the solvent to evaporate in dynamic environment, whereas it cost about 150 s to completely volatize in static environment. It meant that the solution evaporated quickly in dynamic environment. Fig. 6 shows the SEM images of porous structures prepared in these two types of environments. As can be found that regular pore structure was formed when the relative humidity is 60% under dynamic environment, and the pore size enlarges from 1.1 to 1.8 μm with the increasing humidity. However, no regular pattern forms at 60% under static environment. The pore size varies from 1.8 to 2.5 μm, which is larger than that of the pores fabricated in flowing atmosphere.

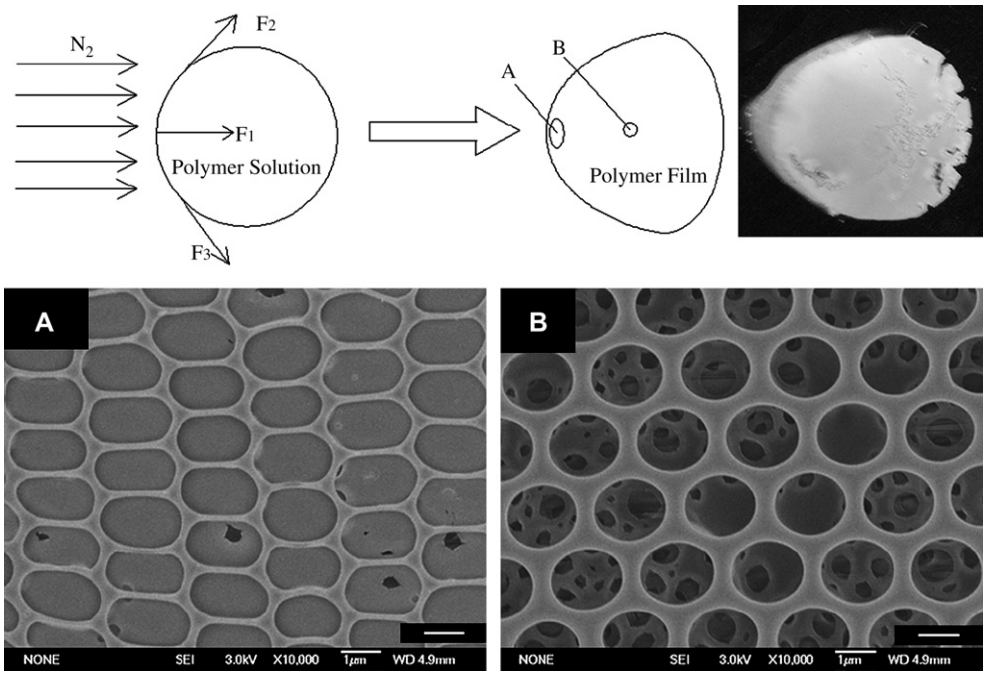

Fig. 5. SEM images of the deformed honeycomb structures at the blowing velocity of 60 m/min. Conditions: temperature, 25 °C; concentration, 2 g/L; spreading volume, 100 μL. The aspect ratio of the elliptic pores is A 1.70, B 1.06. The scale bar is 1 μm.

Simultaneously, pores fabricated under static conditions are less regular than those formed in flowing atmosphere.

It was reported that the capillary attractive forces were important factors during the formation of the honeycomb structure [37]. It was also indicated that the capillary force only acted locally [8,19]. Peng et al. [18] deduced that at the first stage of the solvent evaporation, water droplets condensed on the surface of the solution and formed many isolated 'islands' with ordered structures. These 'islands' were then compactly arranged due to the Marangoni convection

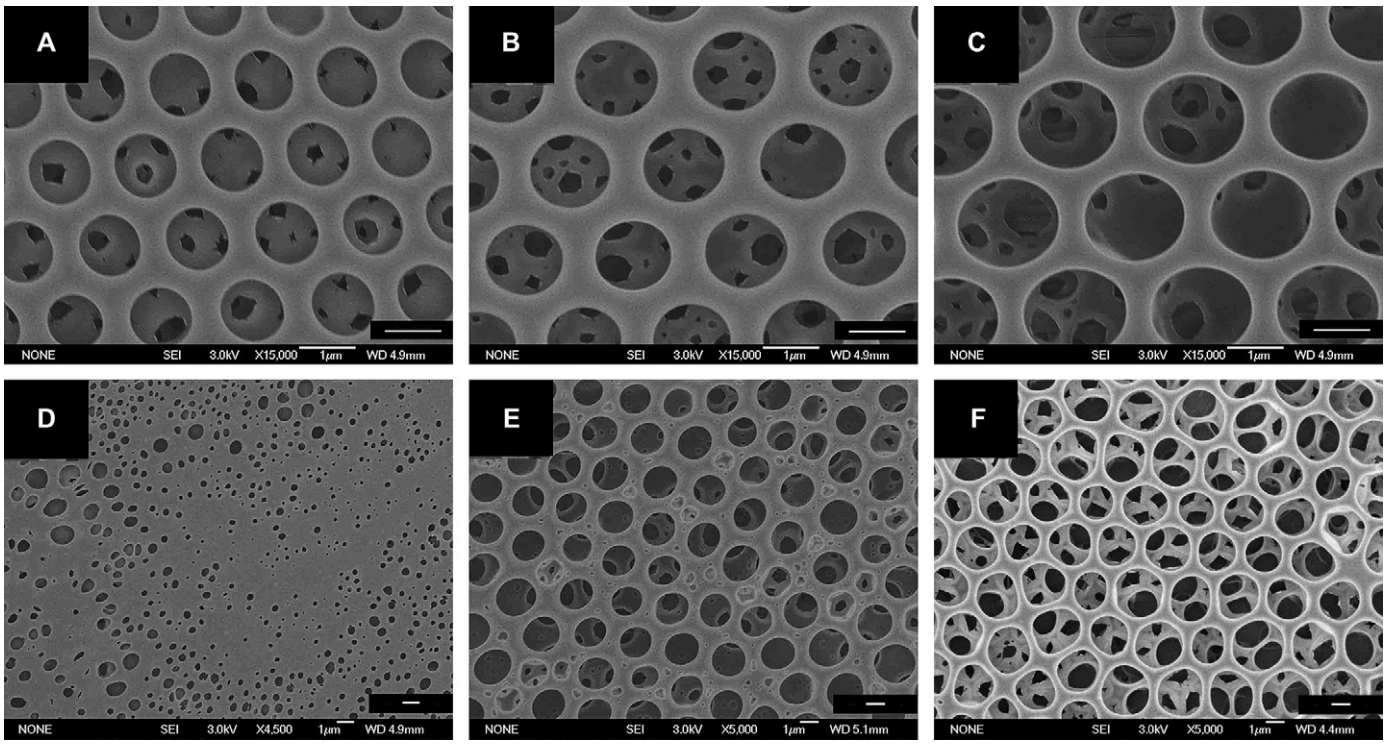

Fig. 6. SEM images of porous structures formed under different environment with various humidity. A–C: under dynamic environment (20 m/min). D–F: under static environment. The relative humidity: A and D: 60%; B and E: 75%; C and F: 85%. Other conditions: concentration, 2 g/L; temperature, 25 °C; spreading volume, 100 μL. The scale bar is 1 μm.

[38–40]. We believed that the neighbor-isolated water droplets were arranged and collided along with Marangoni convection simultaneously. In dynamic environment, the flowing humid air could accelerate the evaporation rate of the solvent. This led to a temperature gradient high enough to cause the condensation of water vapor. Vapor condensed on the surface of the solution and formed many isolated droplets. These many water droplets could occupy most part of the solution surface and close pacing along with the strong Marangoni convection, which was benefited to reduce the collision of the neighboring water droplets and obtain regular patterns (Fig. 6A–C). However, the temperature gradient was small under static humid conditions, leading to a few water droplets and weak Marangoni convection. Water droplets could not closely arrange and form confused patterns (Fig. 6D and E). Therefore, under static conditions, only with higher humid atmosphere could honeycomb structures be fabricated (Fig. 6F). Moreover, under dynamic environment, because airflow accelerated the evaporation rate of the solution, leaving less time for water droplets growing, it could form smaller pore size than those prepared under static environment.

4. Conclusion

A fluorinated polyimide based on a dianhydride monomer 6FDA and a dianiline monomer MDA was synthesized and characterized. The introduction of 6FDA could provide fluorine groups, leading to the increasing solubility of this polyimide. The obtained polyimide kept excellent rigidity and thermal stability, and especially, exhibited good solubility. By dissolving 6FDA–MDA in $CHCl_3$, regular porous structures could be formed in high humid atmosphere. When the airflow blew across the solution surface horizontally, the pores changed their shapes from circle to ellipse. The degree of this change was consistent with the airflow velocity. High velocity led to clear change of the pore morphology. Moreover, because different parts of the film received a shear with different strengths, the deformation of their pores was not uniform. Pores fabricated under flowing atmosphere were smaller and more regular than those formed under static conditions, caused by different evaporation rates of the solution. The dynamic environment could accelerate the evaporating speed of the solvent and made it possible to form regular pore structures in lower humid atmosphere than that of the static environment.

Acknowledgment

This work was financially supported by the National Basic Research Program of China (Grant No. 2003CB615701), which is gratefully acknowledged by the authors.

References

[1] Shimomura M. Prog Polym Sci 1993;18:295–339.
[2] Judith EG, Wijnhoven J, Willeml V. Science 1998;281:802–4.
[3] Tanaka M, Nishikawa K, Okubo H, Kamachi H, Kawai T, Matsushita M, et al. Colloids and Surf A 2006;284–285:464–9.
[4] Nishikawa T, Arai K, Hayashi J, Hara M, Shimomura M. Mater Res Soc Symp Proc 2002;72:229–34. Materials Research Society©.
[5] Yabu H, Shimomura M. Langmuir 2005;21:1709–11.
[6] Widawski G, Rawiso B, François B. Nature 1994;369:387–9.
[7] François B, Pitois O, François J. Adv Mater 1995;7:1041–4.
[8] Pitois O, François B. Eur Phys J 1999;138:225–31.
[9] Pitois O, François B. Colloid Polym Sci 1999;277:574–8.
[10] Jenekhe SA, Chen XL. Science 1999;283:272–5.
[11] Zhao BH, Li CX, Lu Y, Wang XD, Liu ZL, Zhang J. Polymer 2005;46:9508–13.
[12] Stenzel MH. Aust J Chem 2002;55:239–43.
[13] Cheng CX, Tian Y, Shi YQ, Tang RP, Xi F. Macromol Rapid Commun 2005;26:1266–72.
[14] Cheng CX, Tian Y, Shi YQ, Tang RP, Xi F. Langmuir 2005;21:6576–81.
[15] Zhao XY, Cai Q, Shi GX, Shi YQ, Chen GW. J Appl Polym Sci 2003;90:1846–50.
[16] Tian Y, Ding HY, Shi YQ, Jiao QZ, Wang XL. J Appl Polym Sci 2006;100:1013–8.
[17] Tian Y, Liu S, Ding HY, Wang LH, Liu BQ, Shi YQ. Macromol Chem Phys 2006;207:1998–2005.
[18] Peng J, Han YC, Yang YM, Li BY. Polymer 2004;45:447–52.
[19] Xu Y, Zhu BK, Xu YY. Polymer 2005;46:713–7.
[20] Liaw DJ, Liaw BY, Yu CW. Polymer 2001;42:5175–9.
[21] Hergenrother PM, Watson KA, Smith Jr JG, Connell JW, Yokota R. Polymer 2002;43:5077–93.
[22] Fang XZ, Yang ZH, Zhang SB, Gao LX, Ding MX. Polymer 2004;45:2539–49.
[23] Jung MS, Joo WJ, Choi BK, Jung HT. Polymer 2006;47:6652–8.
[24] Yabu H, Tanaka M, Ijiro K, Shimomura M. Langmuir 2003;19:6297–300.
[25] Xie K, Liu JG, Zhou HW, Zhang SY, He MH, Yang SY. Polymer 2001;42:7267–74.
[26] Myung BY, Ahn CJ, Yoon TH. Polymer 2004;45:3185–93.
[27] Wang LH, Zhao ZP, Li JD, Chen CX. Eur Polym J 2006;42:1266–72.
[28] Li HS, Liu JG, Wang K, Fan L, Yang SY. Polymer 2006;47:1443–50.
[29] Yang CP, Su YY, Wen SJ, Hsiao SH. Polymer 2006;47:7021–33.
[30] Hsiao SH, Yang CP, Huang SC. Eur Polym J 2004;40:1063–74.
[31] Tian Y, Jiao QZ, Ding HY, Shi YQ, Liu BQ. Polymer 2006;47:3866–73.
[32] Tian Y, Ding HY, Jiao QZ, Shi YQ. Macromol Chem Phys 2006;207:545–53.
[33] Nishikawa T, Nonomura M, Arai K, Hayashi J, Sawadaishi T, Nishiura Y, et al. Langmuir 2003;19:6193–201.
[34] Li J, Peng J, Huang WH, Wu Y, Fu J, Cong Y, et al. Langmuir 2005;21:2017–21.
[35] Srinivasarao M, Collings D, Philips A, Patel S. Science 2001;292:79–83.
[36] Bolognesi A, Mercogliano C, Yunnus S, Cicardi M, Comoretto D, Turturro A. Langmuir 2005;21:3480–5.
[37] Maruyama N, Karthaus O, Ijiro K, Shimomura M, Koito T, Nishimura S, et al. Supramol Sci 1998;5:331–6.
[38] Maillard M, Motte L, Ngo AT, Poleni MP. J Phys Chem B 2000;104:11871–7.
[39] Maillard M, Motte L, Poleni MP. Adv Mater 2001;13:200–4.
[40] Stowell C, Korgel BA. Nano Lett 2001;1:595–600.